ASAP, a human microtubule-associated protein required for bipolar spindle assembly and cytokinesis

Jean-Michel Saffin*, Magali Venoux*, Claude Prigent†, Julien Espeut‡, Francis Poulat*, Dominique Giorgi*, Ariane Abrieu‡, and Sylvie Rouquier*§

*Institut de Génétique Humaine, Centre National de la Recherche Scientifique, Unité Propre de Recherche 1142, Rue de la Cardonille, 34396 Montpellier Cédex 5, France; †Centre National de la Recherche Scientifique, Unité Mixte de Recherche 6061 Génétique et Développement, Groupe Cycle Cellulaire, Equipe Labellisée LNCC, Université de Rennes I, Institut Fédératif de Recherche 140, 2 Avenue du Pr Léon Bernard, 35043 Rennes, France; and ‡Centre de Recherche de Biochimie Macromoléculaire, Centre National de la Recherche Scientifique Formation de Recherche en Évolution 2593, 1919 Route de Mende, 34293 Montpellier Cédex 5, France

Edited by J. Richard McIntosh, University of Colorado, Boulder, CO, and approved June 13, 2005 (received for review February 4, 2005)

We have identified a unique human microtubule-associated protein (MAP) named ASAP for ASter-Associated Protein. ASAP localizes to microtubules in interphase, associates with the mitotic spindle during mitosis, localizes to the central body during cytokinesis and directly binds to purified microtubules by its COOH-terminal domain. Overexpression of ASAP induces profound bundling of cytoplasmic microtubules in interphase cells and aberrant monopolar spindles in mitosis. Depletion of ASAP by RNA interference results in severe mitotic defects: it provokes aberrant mitotic spindle, delays mitotic progression, and leads to defective cytokinesis or cell death. These results suggest a crucial role for ASAP in the organization of the bipolar mitotic spindle, mitosis progression, and cytokinesis and define ASAP as a key factor for proper spindle assembly.

mitosis

Division of the cell requires coordination between chromosome segregation by a bipolar microtubule (MT)-based structure, the mitotic spindle, and cleavage of the cell by the cytokinetic apparatus. The transition from interphase to mitosis or meiosis is accompanied by a dramatic reorganization of the MT cytoskeleton. The assembly of bipolar spindles is preceded by the movement of centrosomes toward opposite poles of the cell, where these structures function as nucleation sites for MT polymerization (1–3). Spindle assembly and chromosome segregation require MT motor proteins including kinesin-like proteins and cytoplasmic dynein, nonmotor MT-associated proteins (MAPs) required for the regulation of MT dynamics and other molecules, including the small GTPase Ran involved in MT polymerization during mitosis (2, 3). Proper assembly and function of the bipolar spindle is essential for genomic stability (1), and identification of key factors involved in this process as well as knowledge of their regulation are crucial.

To ensure high-fidelity DNA transmission during cell division, both chromosome segregation and cytokinesis must be tightly coordinated. Cytokinesis is accomplished by the contraction of an acto-myosin ring that leads to daughter cell separation at the midbody (4). A number of studies have suggested that the temporal and spatial organization of the cytokinetic machine is under the control of the mitotic spindle (5). The spindle midzone composed of highly bundled MTs, originating from the opposite poles, plays an essential role in the initiation and completion of cell cleavage, and is the binding site for a number of proteins that play a part in cytokinesis (6). Among these proteins are passenger proteins (7–9), protein kinases (10), MT motor proteins (11, 12), and MAPs (13). However, the mechanism of central spindle assembly, the molecular basis for maintenance of the midzone MT bundle and the functional roles of these midzone-associated proteins are still largely unknown. Thus, identification of previously undescribed factors involved in both mitosis and cytokinesis may shed light on these different mechanisms.

In this paper, we report the identification of ASAP, a unique human MAP with no significant homology to proteins of known function, that directly binds to MTs. ASAP colocalizes with MTs in interphase, becomes associated with the mitotic spindle and spindle poles, and localizes to the central body and the residual body during late mitosis and cytokinesis, respectively. We show that its overexpression impedes the formation of a normal bipolar mitotic spindle. We demonstrate that ASAP is an essential factor for successful completion of mitosis, as depletion of ASAP from cells by RNA interference delays mitotic progression and results in a defective cytokinesis or cell death. Thus, we identified a vertebrate spindle-associated protein required for spindle function, mitotic progression, and cytokinesis.

Materials and Methods

Cloning of ASAP cDNA. A partial cDNA clone coding for the human ASAP was obtained from the I.M.A.G.E. Consortium (RZPD, Berlin) and fully sequenced on both strands. Because no stop codon was found, we performed successive RACE by using Marathon-ready cDNA from human fetal brain (Clontech) and oligonucleotides corresponding to the 3′ region of the cDNA (FIS-2F: 5′-TCAGCAGACCATGTGACTAC-3′, then FIS-5F: 5′-TAGCATCATTTGAGGCCTGG-3′). A 750-bp fragment was amplified, subcloned into the TA cloning vector (Invitrogen), and sequenced. This fragment contained a stop codon (TGA) in-frame with the rest of the ORF. In parallel, an EST analysis using the programs of the Wellcome Trust Sanger Institute (www.ensembl.org/genome/central) and the BLAT search program (http://genome.cse.ucsc.edu) was performed. Three overlapping ESTs were found, with one clone 380 bp longer than the clone isolated by RACE-PCR. A full cDNA clone was reconstructed by PCR and cloned into a TOPO-TA cloning vector.

Cell Culture and Transfections. HEK-293 and U-2 OS cells were routinely grown in DMEM (GIBCO/BRL) supplemented with 10% FCS, 0.3 g/liter L-glutamine, 0.05 g/liter streptomycin, and 50,000 units/liter penicillin. Transient transfections were carried out by using JetPEI (QBiogene).

Plasmids, Antibodies, and Reagents. The following recombinant plasmids were constructed: pEYFP-ASAP (pEYFP-C1 vector; EYFP, enhanced yellow fluorescent protein) (Clontech) and ASAP-EGFP (pEAK10-GFP vector) (Edge Biosystems, Gaithersburg, MD). Myc-ASAP and FLAG-ASAP (pRK5 vector). Truncation mutants were constructed in pEYFP-C1 and pEAK-EGFP.

For immunofluorescence studies, monoclonal antibodies to

This paper was submitted directly (Track II) to the PNAS office.

Abbreviations: MT, microtubule; MAP, MT-associated protein; YFP, yellow fluorescent protein; EYFP, enhanced YFP; PFA, paraformaldehyde; siRNA, small interfering RNA.

Data deposition: The sequence reported in this paper has been deposited in the GenBank database (accession no. AY690636).

§To whom correspondence should be addressed. E-mail: rouquier@igh.cnrs.fr.

α-tubulin (Sigma), centrioles (GT-335), and rabbit polyclonal antibodies to γ-tubulin (Sigma) and survivin (R & D Systems) were used at dilutions 1:1,000, 1 :10,000, 1:1,000, and 1:200, respectively. Nocodazole and Hoechst dye 33258 were purchased from Sigma.

Immunofluorescence and Microscopy. Cells were fixed for 4 min in methanol at −20°C or in 4% paraformaldehyde (PFA) at room temperature for 10 min followed by permeabilization in 0.1% Triton X-100. In some cases, for a better visualization of MT cytoskeletons, cells were fixed in 3% PFA/0.25% glutaraldehyde, extracted in 0.2% PHEM–Triton X-100 before cold methanol fixation, or prefixed with DSP before extraction and fixation in DSP-PFA as indicated in ref. 14. Fixed cells were incubated for 1 h at 37°C with the primary antibody, and 30 min at 37°C with the secondary antibody. Fluorochromes were Alexa Fluor 488, Alexa Fluor 546, and Alexa Fluor 594 dyes (Molecular Probes). Cells were mounted and observed at room temperature on a Leica DMRA2 fluorescence microscope or on a Leica TCS SP2 confocal microscope. Images were acquired respectively with the METAVUE or LCS LEICA confocal software and manipulated with PHOTOSHOP (Adobe Systems, San Diego).

Western Blotting. Cells were washed with PBS and scraped in lysis buffer (50 mM Tris, pH 8.0/120 mM NaCl/5 mM EDTA/0.5% Nonidet P-40) supplemented with 1 mM DTT and a protease inhibitor mixture tablet (Roche Diagnostics). Total proteins transferred to filters were detected by various antibodies and visualized by enhanced chemiluminescent reagents (ECL^+, Amersham Pharmacia).

Generation and Affinity Purification of Polyclonal ASAP Antibodies. Polyclonal rabbit serum to the full-length human protein or to the C-terminal-deleted protein (ASAP-ΔCTer, amino acids 1–420) were raised against the corresponding GST fusion protein purified from bacteria *Escherichia coli* $BL21RP^+$. The antibodies were affinity purified on a GST column followed by a GST-ASAP fusion protein affinity column. Antibodies were routinely used at 1:500 for immunofluorescence and 1:10,000 for Western blots.

Microtubule-Binding Assays. GST-ASAP or GST-ASAP-ΔCter (1 μg/μl) were incubated for 30 min at room temperature in BRB80 buffer (80 mM K-Pipes/1 mM $MgCl_2$/1 mM EGTA) with 5 μM taxol-stabilized tubulin or buffer (input). The reaction was then centrifuged for 30 min at 37°C through a 40% glycerol-BRB80 cushion at 50,000 × *g* to separate MT-associated from soluble proteins. The same experiment was done by using various concentrations of tubulin to determine the dissociation constant. Percentage of ASAP bound to MTs was quantified by using the IMAGEJ freeware (National Institutes of Health), and results were plotted by using the saturation binding curve of PRISM (GraphPad, San Diego) to determine the K_d.

Small Interfering RNA (siRNA) Oligonucleotides and Transfection. For ASAP siRNA, the following target sequence was used: $_{642}$CGCCGAAUGGCAUACAAUU$_{660}$. Duplexes were transfected either once or twice 24 h apart in U-2O S cells by using Oligofectamine (Invitrogen) in accordance with the supplier's recommendations. Cells were collected 24, 48, or 72 h after transfection. In some cases, cells were synchronized by double thymidine block and transfected as described (9). A scrambled siRNA of ASAP (5′-CAAGUUACGCGGUUACCAAUU-3′) was used as a control. An ASAP mutant not responsive to the siRNA was obtained by changing the coding sequence of the FLAG-ASAP construct by PCR-based mutagenesis within the siRNA-targeted sequence at two wobble bases, without affecting the encoded amino acids. For movies, U-2 OS cells were treated as described above. Four hours after the transfection, cells were followed by time-lapse microscopy. Synchronized and siRNA-transfected U-2 OS stably expressing H2B-GFP were followed upon the first round of mitosis, 12 h after release. Phase contrast, differential interference contrast, or fluorescent image data sets were collected every 5 min for 24–36 h.

Results

Molecular Characterization of ASAP. In the course of a screen to identify new proteins implicated in intracellular traffic, we isolated a human sequence that shows ≈22% sequence identity over 250 aa of its C terminus with human MAP1A, but no significant homology with any other known proteins. No full-length human cDNA sequence was available in public databases, probably because of a dA-rich region in its 3′ end. We cloned a full-length human cDNA sequence, using a combination of partial ESTs and 3′ RACE-PCR strategy. The cDNA contains a single ORF of 2,361 bp predicted to encode a protein of 647 aa with a molecular mass of ≈75 kDa and an isoelectric point of 8.9. Based on the currently compiled genome sequence, the human gene is encoded by 13 exons and is located on chromosome 4q32. The encoded protein was named ASAP (see below). Database searches with either the nucleotide or the predicted protein sequences did not identify any known protein that shares global homology. However, BLAST searches identified a conserved potential homologue from mouse (mASAP, 647 aa, 75% sequence identity) and few partial *Xenopus* ESTs (≈55% identity). No clear homolog could be identified in invertebrates. ASAP contains two potential nuclear localization signals, two predicted coiled-coil domains (amino acids 297–327 and 477–628), and a number of predicted phosphorylation sites, but no other identifiable functional motifs.

To investigate the possibility that ASAP functions as a MAP, we raised polyclonal antibodies against both the full-length protein, anti-ASAP, and the truncated form deleted in the MAP coiled-coil domain, anti-ASAP-ΔCter. Both affinity-purified antibodies recognized a single protein band of ≈110 kDa in HEK-293 or U-2 OS cells, showing a higher molecular weight than the predicted. This difference may be partially accounted by posttranslational modifications and/or conformation issues. The specificity of the antibodies was assessed by comparing these profiles to that observed with the anti-FLAG antibody against FLAG-ASAP-transfected cells (Fig. 1*A*). Further immunofluorescence analyses on endogenous or overexpressed ASAP experiments were always done in parallel on two cell lines: HEK-293 and U-2 OS. The main phenotypes were observed in both cell lines.

ASAP Is a MAP. We next analyzed the subcellular localization of endogenous ASAP. Unfortunately, the four antibodies generated against ASAP or ASAP-ΔCTER gave a significant background in immunofluorescence studies. The same ASAP localization was observed by using several fixation methods. Cells directly fixed in PFA showed more integer ASAP and that MT integrity was affected, whereas the contrary was observed with the other fixation methods. Because of looking at the subcellular localization of ASAP, we chose to use PFA fixation. Immunofluorescence studies in PFA-fixed cells costained for ASAP and α-tubulin demonstrated that, in interphase, endogenous ASAP localizes to the cytoplasm in a filamentous-like pattern, suggestive of binding to MTs. ASAP undergoes dramatic redistribution during mitosis. It first relocates to the poles at the astral MTs (based on this localization, we named the protein ASAP for ASter-Associated Protein) and the spindle during prometaphase, metaphase, and early anaphase, then to centrosomal MT asters and the central spindle during anaphase and early telophase. During late cytokinesis, ASAP colocalizes with the midzone MT bundles when it is also located on MTs nucleated from centrosomes. Confocal analysis of cells costained for ASAP and α-tubulin shows colocalization with interphase, mitotic, and midzone MT arrays (Fig. 1*B*).

Immunofluorescence studies suggested that ASAP is expressed constitutively during the cell cycle. We confirmed this

CELL BIOLOGY

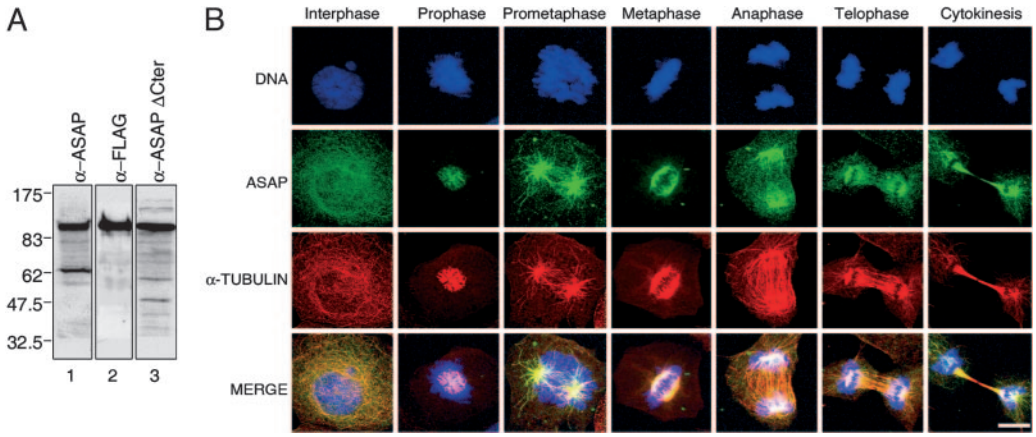

Fig. 1. Characterization of ASAP. (*A*) Characterization of anti-human ASAP antibodies by immunoblotting. The specificities of the affinity-purified anti-ASAP and anti-ASAP-ΔCter antibodies were assessed by using cell extracts from U-2 OS, and compared to the profile observed with the anti-FLAG antibody against FLAG-ASAP transfected U-2 OS cells (lane 2). (*B*) Subcellular localization of endogenous ASAP during the cell cycle. Exponentially growing U-2 OS were fixed with PFA and processed for immunofluorescence with the affinity-purified antibody against ASAP (green) and an antibody against α-tubulin (red). DNA was stained with Hoechst dye 33258 (blue). (Bar, 10 μm.)

observation by monitoring the protein expression throughout a synchronously growing population of U-2 OS (data not shown).

Coimmunolocalization of ASAP with the MT network in interphase and mitosis prompted us to suggest that ASAP might be a MAP. Sequence analysis suggested that the C terminus of ASAP might contain the MT-binding domain. We studied whether ASAP or ASAP-ΔCter interacts with pure prepolymerized MTs in a sedimentation assay. A purified recombinant GST-ASAP fusion protein copelleted with taxol-stabilized MTs, indicating that ASAP binds directly to MTs. Deletion of the C-terminal domain strongly reduced the ability of ASAP to copellet with MTs (Fig. 2*A*). To check that endogenous ASAP behaved similarly, a cosedimentation assay was also performed by using whole cell lysates and Taxol-stabilized MTs. A substantial portion of endogenous ASAP was found in the pellet fraction associated with polymerized MTs (data not shown). To estimate the affinity of ASAP for MTs, ASAP was incubated with different concentrations of MTs. Plotting bound ASAP versus the MT concentrations yielded an equilibrium dissociation constant of ≈1 μM (the tubulin concentration required to bind 50% of ASAP; Fig. 2*B*), indicating MT binding with a moderately high affinity. Overall, these results demonstrate that ASAP colocalizes with, and directly binds to, MTs via its MAP C-terminal domain.

To study the effect of gain of ASAP functions, full-length EGFP-(C terminus)-, EYFP-(N terminus)-, FLAG epitope-(N terminus)-, or MYC epitope-(N terminus)-tagged versions of ASAP were overexpressed in HEK-293 and U-2 OS cells. By Western blot, EGFP or EYFP constructs were expressed at ≈135 kDa and FLAG or MYC constructs were expressed at ≈110 kDa (Fig. 2*C*). All four recombinant proteins showed similar intracellular patterns. ASAP-ΔCter was coupled either to EYFP (N terminus) or EGFP (C terminus). The two constructs expressed the proteins at the expected sizes and at similar levels as assessed by Western blot analysis (Fig. 2*C*).

As observed for the endogenous protein, overexpressed ASAP localized to the cytoplasm in a filamentous-like pattern in interphase, and to both half spindles in mitotic cells. Colocalization of ASAP and MTs was confirmed in interphase and metaphase by costaining the cells with an anti-α-tubulin antibody. ASAP overexpression induced a striking formation of thick, perinuclear rings of MTs (more important in the U-2 OS cell line), suggesting a function in MT network organization. ASAP and α-tubulin colocalized to these rings (Fig. 2*D*). Similar bundled rings have been observed after overexpression of other MAPs in mammalian culture cells (13, 15, 16). When ASAP-ΔCter was overexpressed, the fiber-like distribution of ASAP was lost in interphase. This overexpression does not promote MT bundling, suggesting that this property requires the MT binding domain (Fig. 2*D*). Thus, when overexpressed, ASAP has the capacity to rearrange and stabilize MT arrays. To test this hypothesis, we determined whether ectopic expression of ASAP can protect MTs from depolymerization by nocodazole. U-2 OS cells expressing either EGFP or EGFP-tagged ASAP were analyzed by immunofluorescence. GFP did not affect nocodazole-induced MT depolymerization. In contrast, bundled MTs were extremely stable in EGFP-ASAP transfected cells, and did not depolymerize in the presence of high doses of nocodazole (Fig. 2*E*). These results suggest that ASAP can stabilize MTs *in vivo*.

Both overexpressed exogenous protein and endogenous ASAP colocalize with interphase and mitotic MTs. Thus, ASAP fulfills the criteria of a bona fide MAP that associates, reorganizes and stabilizes MTs.

Overexpression of ASAP Leads to Monopolar Spindle Formation. One of the main consequences of the overexpression of ASAP was that it prevented many cells from completing cytokinesis (Fig. 3). In HEK-293 cells, we observed an increase in both the appearance of multinucleated cells (≈12% of the transfected cells) and the mitotic index (≈24% in transfected cells versus ≈8% in nontransfected control cells). Among these mitotic cells, 76% displayed one large MT aster (monopolar spindle) emanating from a single organizing center (Fig. 3 *A* and *B*). Bright circular filaments that resemble stabilized MT observed in interphase surrounded some of these monopolar spindles (Fig. 3*A Upper*). ASAP appeared to be more restricted to the center of the astral MTs, i.e., toward the minus end of the MTs (Fig. 3*A Lower*). A few mitotic cells containing multipolar spindles were also observed. Overexpression of ASAP in U-2 OS cells also resulted in an accumulation of cells in mitosis with a comparable proportion of cells with monopolar spindles (>70%), but fewer multinucleated cells were observed. FACS analysis of ASAP-transfected U-2 OS cells showed ≈40% in G_2/M compared to 17% in the mock control (data not shown). We then immunostained ASAP and the GT335 antigen, a well characterized marker of centrioles, by using a monoclonal antibody directed against glutamylated tubulin (17). Multinucleated cells showed centrosome amplification suggestive of cytokinesis failure (Fig. 3*C*). Moreover, each MT aster (in monopolar or multipolar spindles) always contained several centrioles. Monopolar spindles frequently con-

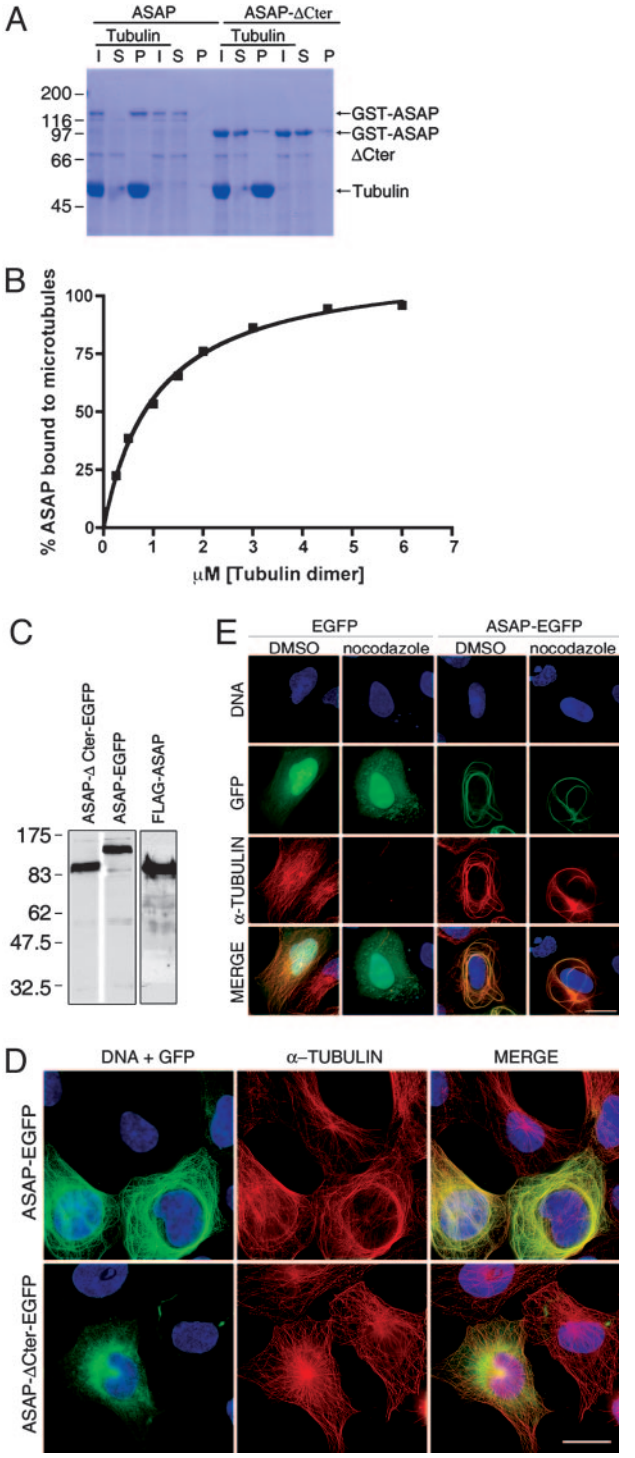

Fig. 2. ASAP is a MAP. (*A*) MT sedimentation assay of the GST-ASAP or GST-ASAP-Δ Cter recombinant proteins with or without pure prepolymerized MTs (I, input; S, supernatant; P, pellet). Proteins were resolved on an SDS/10% PAGE electrophoresis gel and visualized by Coomassie blue staining. (*B*) Affinity of ASAP for MTs was determined by plotting the percentage of ASAP bound to MTs versus the tubulin dimer concentration yielding a dissociation constant (K_d) of ≈1 μM. (*C*) Immunoblot of ASAP-ΔCTER-EGFP, ASAP-EGFP, or FLAG-ASAP transfected U-2 OS cells obtained by using an anti-GFP or an anti-FLAG antibody, respectively. (*D* and *E*) Forty-eight hours after transfection with 2 μg of ASAP-EGFP, ASAP-ΔCTER-EGFP (*D*) or EGFP (*E*) U-2 0S cells were fixed with DSP-PFA and labeled with Hoechst dye 33258 (blue) for DNA and an anti-α-tubulin antibody (red). In *E*, cells were treated with 10 μM nocodazole for 3 h. GFP signals are in green. (Bars, 20 μm.)

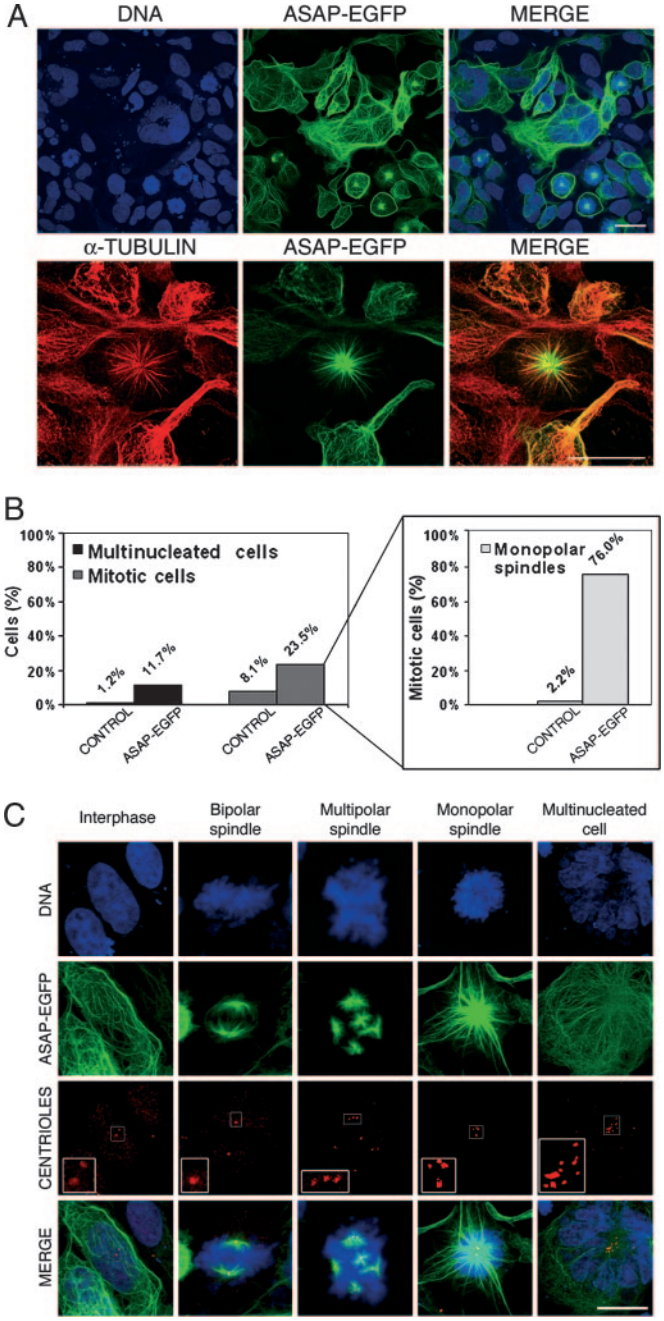

Fig. 3. Overexpression of ASAP leads to monopolar spindle formation. Forty-eight hours after transfection with 2 μg of ASAP-EGFP, HEK-293 cells were fixed with PFA. (*A*) (*Upper*) DNA was labeled with Hoechst dye 33258. (*Lower*) Enlargement of a monopolar spindle: cells were stained with anti-α-tubulin (red). GFP signals are in green. (*B*) Quantitation of multinucleated, mitotic, and monopolar mitotic cells. For each sample, 300 cells were examined by microscopy. Transfected cells were scored and compared to nontransfected cells (control). Among the mitotic cells, monopolar spindles were quantified (*Inset*). (*C*) Cells were labeled with Hoechst dye 33258 and an anti-GT335 (centrioles) (red). *Insets* show a higher magnification of GT-335 foci. (Bars, 20 μm.)

tained four centrioles. A γ-tubulin staining revealed the presence of two centrosomes (data not shown). These results indicate that the centrosome had clearly duplicated, but had failed to separate sufficiently to form a bipolar spindle (Fig. 3*C*). Thus, overexpression of ASAP inhibited centrosome separation leading to monopolar spindle formation and cytokinesis defects. Interestingly, the

truncated form of ASAP lacking the MT-binding domain failed to induce these phenotypes, indicating that binding to MTs is a prerequisite. These data provide evidence that overexpression of ASAP can interfere with mitotic progression in human cells as it is generally observed with any factor that disrupts normal spindle assembly, and confirms that ASAP is a MAP.

Finally, overexpression of mouse ASAP produced the same phenotype as human ASAP. The same mitotic defects were observed by overexpressing mouse ASAP in the nontransformed mouse NIH 3T3 cell line (data not shown).

Depletion of ASAP by RNA Interference Delays Mitotic Progression and Causes Failure of Cytokinesis. To gain deeper insight into the function of ASAP in mitosis, gene silencing siRNA was used in the U-2 OS cell line. Cells were transfected once or twice 24 h apart with ASAP siRNA and observed for 24–72 h. The phenotype observed 48 h after a double dose of siRNA was the same as that observed 72 h after a single dose. Starting 24 h after the single transfection, the level of ASAP protein was reduced by at least 90% as shown by Western blot and immunofluorescence analyses, suggesting that ASAP was almost completely depleted in most cells, whereas α-tubulin was unaffected. Mock or scrambled siRNA control transfections did not affect the expression of ASAP (Fig. 4 *A* and *B1*). After 24 h, the percentage of fixed mitotic cells was higher in ASAP-depleted cells than in the control (15% versus 11%), it was approximately the same after 48 h (14.7% versus 14%) and significantly lower after 72 h (2.5% versus 8%). This difference could reflect the fact that depletion of ASAP is lethal, resulting in the detachment and loss of many transfected cells. Indeed, compared to the controls, ASAP-depleted transfections showed a significant reduction in cell number after 24 h, and very few viable cells were detected after the last time point (≈80 h after transfection). The interphase ASAP-depleted cells presented an apparently normal MT network. However, ≈68% of ASAP-depleted cells (versus 7.5% in the control) showed abnormal spindles, frequently associated with an altered pattern of chromosome alignment in metaphase (Fig. 4*B*). However, a prominent failure in cytokinesis was observed in ASAP-depleted cells, as shown by staining for survivin, a marker of the mid-body during telophase/cytokinesis (Fig. 4*C* and Fig. 5*A*, which is published as supporting information on the PNAS web site). We observed a cytoplasmic bridge of α-tubulin remaining between the two daughter cells. The presence of this cytoplasmic bridge was confirmed by an observation of the cells under white light (Fig. 5*A3*). We used the survivin-positive cells to score for telophase/cytokinesis, assuming that the survivin-negative cells (but those with a long cytoplasmic bridge) had aborted cytokinesis and returned to interphase (data not shown). To prove that the phenotypes observed after ASAP-siRNA were indeed caused by specific knockdown of the ASAP protein, we performed a rescue experiment by cotransfecting a vector expressing an ASAP cDNA containing two silent mutations within the ASAP sequence recognized by the siRNA (ASAP-SIL). When cotransfected with the ASAP-siRNA, ASAP-SIL labeled aster (Fig. 4*B1*) and cytoplasmic MTs (data not shown). About 10.5% of cells showed abnormal spindles (Fig. 4*B2*), and ≈8% were observed in cytokinesis after 72 h, demonstrating the restoration of normal function (Fig. 4*C2*).

The other main feature of ASAP-depleted cells was an accumulation in prometaphase/metaphase mitotic cells observed in the first round of mitosis after release of synchronized transfected cells or after 24 h (see below).

Knockdown of ASAP also altered nuclear morphology in interphase cells: 26% of ASAP-depleted cells displayed smaller and invaginated or deformed nuclei (Fig. 5*C*) as well as mininuclei (data not shown). γ-tubulin staining of ASAP-depleted cells revealed no abnormal centrosome number (data not shown).

Preliminary time-lapse experiments revealed that ASAP-depleted cells were severely delayed during mitosis. We determined

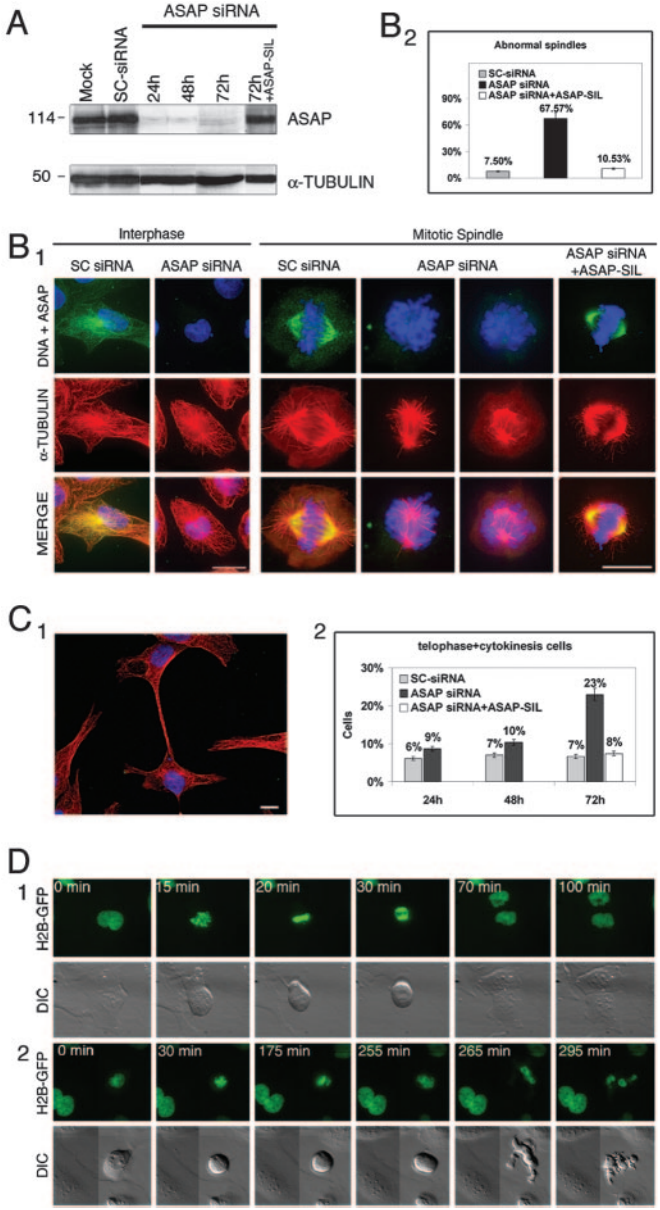

Fig. 4. Inhibition of ASAP expression leads to abnormal spindles and cytokinesis defects (*A–D*). U-2 OS cells were treated with siRNA duplexes ASAP or scrambled (SC). (*A*) Immunoblot demonstrating depletion of ASAP after 24, 48, or 72 h. In the last lane, 2 μg of ASAP-SIL vector was cotransfected. Total U-2 OS cell extracts were probed with the antibodies indicated on the right side of the panel. Antibodies to α-tubulin were used to demonstrate equal loading. Molecular masses are given in kDa. (*B* and *C*) Immunofluorescence after 72 h of U-2 OS SC and ASAP-siRNA transfections. Cells were DSP-PFA-fixed (*B*) or PFA-fixed (*C*) and costained with anti-ASAP (green) and anti-α-tubulin (red) antibodies and Hoechst dye 33258 (blue). (*B1*) Immunofluorescence demonstrating depletion of ASAP in ASAP-siRNA transfected cells compared to the SC-siRNA transfected cells. ASAP-siRNA transfected cells show abnormal spindles (*B1*), long tubulin bridges (*C1*). (Bars, 20 μm.) (*B2*) Quantification of abnormal spindles 24–48 h after transfection. Data were obtained from three independent experiments ($n = 3$) (total number of cells scored: SC-siRNA, 40; ASAP-siRNA, 37; ASAP-siRNA+ASAP-SIL, 38). (*C2*) Quantitation of telophase/cytokinesis cells relative to total cell number, ($n = 3$) (total number of cells scored: SC-siRNA-24h, 567; SC-siRNA-48h, 780, SC-siRNA-72h, 352; ASAP-siRNA-24h, 666; ASAP-siRNA-48h, 1,462; ASAP-siRNA-72h, 256; ASAP-siRNA-72h+ASAP-SIL, 147). (*D*) Live imaging of ASAP-depleted H2B-GFP U-2 OS cells reveals defects in chromosome congression and segregation. Synchronized cells were transfected with SC or ASAP-siRNA and followed by time-lapse since entering mitosis. (*D*) Selective frames of H2B-GFP U-2 OS cells transfected with SC-siRNA (*D1* and Movie 2) or ASAP siRNA (*D2* and Movie 3).

that 80% of ASAP-depleted cells are delayed in mitosis for three times longer than control, whereas the remaining 20% of ASAP-depleted cells do not divide for >10 h (against 49 min in control cells; Fig. 6*A* and Movie 1, which are published as supporting information on the PNAS web site). These prolonged mitosis eventually aborted and resulted in cellular death for about one-third of ASAP-depleted cells and was often accompanied by multiple membrane protrusion (blebbing) typical of dying cells (18). Other ASAP-depleted cells were clearly failing cytokinesis. To investigate the effects of ASAP depletion on mitotic chromosome dynamics, we examined synchronized U-2 OS cells expressing histone H2B-GFP and treated by ASAP siRNA. None of the 17 cells followed by time-lapse completed mitosis normally. We observed prolonged prometaphase and metaphase. Cells were unable to align their chromosomes on a normal metaphase plate, then underwent multipolar anaphase and/or defective chromosome segregation (Figs. 4*D* and 6 *B–D* and Movies 2–6, which are published as supporting information on the PNAS web site) leading to cell death. None of the 15 observed control cells exhibited any of these defects and all exited mitosis normally. This failed mitosis could explain the defects in nuclear morphology observed by immunofluorescence.

Discussion

Here, we describe the characterization of ASAP, a human protein that defines a unique family of vertebrate MAPs. Native and recombinant ASAP bind to MTs via the C-terminal domain. ASAP colocalizes with MTs at all stages of the cell cycle, strongly suggesting that this protein might play a role in the regulation of MT dynamics and in the stabilization of the MT network during both mitosis and interphase.

Three phenotypes have been clearly observed when the level of ASAP protein was perturbed. (*i*) In interphase, overexpression of ASAP induces the formation of thick bundled MTs resistant to depolymerization by nocodazole. This observation suggests that ASAP possesses strong stabilizing effect on MTs, like some other cytoplasmic and mitotic MAPs (19).

(*ii*) The most striking phenotype observed after ASAP overexpression is an increased mitotic index. An excess of ASAP gives rise to multipolar and mainly monopolar spindles with grouped centrosomes indicating that the protein is required for bipolar spindle assembly. How and when ASAP is needed remains to be clarified. Defects in the mechanisms involved in separation or maturation of centrosomes can lead to mitotic monoaster of MTs. If the two daughter cells cannot separate, they often generate binucleated cells that will also give rise to multipolar and monopolar spindles in the next mitosis. Several mitotic protein kinases [for example Cdk1 (20), Nek2A (21), Polo (22), and Aurora A (23)] are involved in the control of such mechanisms and can lead to similar phenotypes when deregulated. The phenotypes observed could then reflect either a defect of ASAP regulation by such kinase(s) or the fact that ASAP overexpression dominantly perturbs the normal activity of one of these regulatory kinases.

(*iii*) The predominant early consequence of ASAP depletion is cell death, probably induced by the accumulation of mitotic defects. Time-lapse analysis of ASAP-depleted cells showed that ASAP is required for successful passage through mitosis. In the absence of ASAP, cells show abnormal spindles and a mitotic delay (mitosis lasts at least three times longer in cells lacking ASAP than in control cells). It is precisely the progression through prometaphase/metaphase that is prolonged, and this correlates with chromosome congression defects followed by chromosome segregation defects. In fact, many cells do not survive this defect; most of them were found dead after ASAP siRNA treatment. Some cells survive this prolonged mitosis but fail cytokinesis as observed later on fixed cells and time-lapse experiments. Either they eventually exit mitosis by escaping the checkpoints ("mitotic slippage" process; ref. 24) and the phenotype observed indicates that ASAP is also required for cytokinesis, or they contain sufficient residual ASAP to manage to pass through mitosis but eventually fail cytokinesis. Although most reported examples of cytokinesis failures involve furrow regression and cell binucleation sometimes inducing cell death, there are a few examples of abortive cytokinesis in which daughter cells remain connected by bridge-like cytoplasmic structures like those found in ASAP-depleted cells (e.g., siRNA-annexin depleted cells; ref. 25 and references therein). Coordination of cytokinesis with chromosome congression and segregation is critical for proper cell division. It remains to be clarified whether the cytokinetic defects are a direct effect of ASAP depletion or an indirect consequence of the chromosome congression and segregation defects.

Taken together, our data demonstrate that ASAP is a vertebrate MAP that stabilizes interphase MTs and plays a key role in mitosis. Although gain of function (overexpression) and loss of function (depletion) of ASAP give rise to different phenotypes, they are both complementary and strongly indicate that ASAP plays a crucial role in bipolar spindle assembly, mitosis, and cytokinesis. Consequently, the level of ASAP protein must be tightly regulated in the cell. The mitotic events in which ASAP is involved are essential to ensure accurate chromosome segregation and genome stability. The mitotic defects observed in cells overexpressing ASAP are often seen in tumor cells. Moreover, ASAP depletion induces delay in mitosis followed by a subsequent cell death. Thus, ASAP is an attractive target for drug design in cancer therapy.

We thank Drs. M. Bornens, M. Benkirane, J.-M. Brondello, D. Fesquet, T. Lorca, and D. Maiorano for helpful discussions, Dr. B. Eddé (Centre de Recherche de Biochemie Macromoleculaire, Montpellier, France) for supplying the GT335 antibody, Dr. Alberto Gandarillas for FACS expertise, N. Lautredou for confocal immunofluorescence microscopy, Drs. D. Fisher, Barbara Trask, and Rosemary Kiernan for critical comments on the manuscript, and Dr. M. Méchali for his constant interest in this work. J.-M.S. and M.V. are recipients of Ministère de l'Education, de la Recherche, et de la Technologie fellowships. This work was supported by grants from Association pour la Recherche sur le Cancer and Ligue Nationale contre le Cancer (to S.R.) and Équipe Labellisée LNCC (to C.P.).

1. Compton, D. A. (2000) *Annu. Rev. Biochem.* **69,** 95–114.
2. Karsenti, E. & Vernos, I. (2001) *Science* **294,** 543–547.
3. Wittmann, T., Hyman, A. & Desai, A. (2001) *Nat. Cell Biol.* **3,** E28–E34.
4. Cao, L. G. & Wang, Y. L. (1990) *J. Cell Biol.* **111,** 1905–1911.
5. Maddox, A. S. & Oegema, K. (2003) *Nat. Cell. Biol.* **5,** 773–776.
6. Robinson, D. N. & Spudich, J. A. (2000) *Trends Cell Biol.* **10,** 228–237.
7. Mackay, A. M., Ainsztein, A. M., Eckley, D. M. & Earnshaw, W. C. (1998) *J. Cell Biol.* **140,** 991–1002.
8. Skoufias, D. A., Mollinari, C., Lacroix, F. B. & Margolis, R. L. (2000) *J. Cell Biol.* **151,** 1575–1582.
9. Gassmann, R., Carvalho, A., Henzing, A. J., Ruchaud, S., Hudson, D. F., Honda, R., Nigg, E. A., Gerloff, D. L. & Earnshaw, W. C. (2004) *J. Cell Biol.* **166,** 179–191.
10. Lee, K. S., Yuan, Y. L., Kuriyama, R. & Erikson, R. L. (1995) *Mol. Cell. Biol.* **15,** 7143–7151.
11. Martineau-Thuillier, S., Andreassen, P. R. & Margolis, R. L. (1998) *Chromosoma* **107,** 461–470.
12. Hill, E., Clarke, M. & Barr, F. A. (2000) *EMBO J.* **19,** 5711–5719.
13. Mollinari, C., Kleman, J. P., Jiang, W., Schoehn, G., Hunter, T. & Margolis, R. L. (2002) *J. Cell Biol.* **157,** 1175–1186.
14. Bell, P. B., Jr., & Safiejko-Mroczka, B. (1995) *Scanning Microsc.* **9,** 843–857; discussion 858–860.
15. Koonce, M. P., Kohler, J., Neujahr, R., Schwartz, J. M., Tikhonenko, I. & Gerisch, G. (1999) *EMBO J.* **18,** 6786–6792.
16. Smith, D. S., Niethammer, M., Ayala, R., Zhou, Y., Gambello, M. J., Wynshaw-Boris, A. & Tsai, L. H. (2000) *Nat. Cell. Biol.* **2,** 767–775.
17. Bobinnec, Y., Moudjou, M., Fouquet, J. P., Desbruyeres, E., Edde, B. & Bornens, M. (1998) *Cell Motil. Cytoskeleton* **39,** 223–232.
18. DeLuca, J. G., Moree, B., Hickey, J. M., Kilmartin, J. V. & Salmon, E. D. (2002) *J. Cell Biol.* **159,** 549–555.
19. Drewes, G., Ebneth, A. & Mandelkow, E. M. (1998) *Trends Biochem. Sci.* **23,** 307–311.
20. Mayer, T. U., Kapoor, T. M., Haggarty, S. J., King, R. W., Schreiber, S. L. & Mitchison, T. J. (1999) *Science* **286,** 971–974.
21. Faragher, A. J. & Fry, A. M. (2003) *Mol. Biol. Cell* **14,** 2876–2889.
22. Barr, F. A., Sillje, H. H. & Nigg, E. A. (2004) *Nat. Rev. Mol. Cell. Biol.* **5,** 429–440.
23. Marumoto, T., Zhang, D. & Saya, H. (2005) *Nat. Rev. Cancer* **5,** 42–50.
24. Rieder, C. L. & Maiato, H. (2004) *Dev. Cell* **7,** 637–651.
25. Tomas, A., Futter, C. & Moss, S. E. (2004) *J. Cell Biol.* **165,** 813–822.